

NOTES AND CORRESPONDENCE

Comments on “The k^{-3} and $k^{-5/3}$ Energy Spectrum of Atmospheric Turbulence: Quasigeostrophic Two-Level Model Simulation”

K. SHAFER SMITH

Center for Atmosphere Ocean Science, Courant Institute of Mathematical Sciences, New York University, New York, New York

1 April 2003 and 27 October 2003

1. Introduction

Recently, Tung and Orlando (2003, hereafter TO) proposed a new explanation for the observed spectra of atmospheric turbulence reported originally by Nastrom and Gage (1985). The present comment is intended to expand on some issues not considered explicitly by TO, and to contrast the modeling philosophy taken by TO relative to that implicitly invoked in most numerical quasigeostrophic (QG) studies. In particular, the comment explains why the result of TO has not been seen in previous studies using similar models, and notes some potential pitfalls in the interpretation of the results of TO.

The features of the atmospheric spectrum reported by Nastrom and Gage (1985) are similar to those expected from geostrophic turbulence phenomenology, but nevertheless difficult to describe completely within that framework, assuming a single disturbance source. Tung and Orlando (2003) detail these difficulties and the theories proposed to get around them, and go on to propose the following new hypothesis. Baroclinic instability, they argue, generates turbulent energy in the midlatitude troposphere at scales corresponding to zonal wavenumbers in the range 3–12, resulting in a short upscale cascade of energy (truncated by large-scale Ekman friction and the finite scale of the planet at wavenumber 1), and a downscale cascade of enstrophy, resulting in the k^{-3} spectrum observed down to scales of about 600 km for the zonal wind. Tung and Orlando (2003) further claim that, in contradistinction to basic quasigeostrophic turbulence phenomenology, there is a small downscale cascade of *energy*, and that at some scale k , such that $\epsilon k^2 = \eta$, where ϵ is the downscale energy flux and η is the downscale enstrophy flux, the spectrum due to

the downscale energy flux dominates that due to the direct cascade of enstrophy. The result, they argue, is the appearance of a $k^{-5/3}$ energy spectrum at small scales, due to the small but nonnegligible direct cascade of energy. Using a two-layer spectral quasigeostrophic model, forced by radiative relaxation toward a baroclinically unstable mean state and dissipated at large scale by linear Ekman damping and at small scale by a very high order hyperviscosity ($\nu_s \nabla^s \zeta$, with $s = 18$ and $\zeta = \nabla^2 \psi$), TO obtain results apparently consistent with their hypothesis.

The existence of a small downscale energy flux (and a small upscale enstrophy flux) in geostrophic and two-dimensional turbulence is well-supported by numerical evidence (I have seen it in my own simulations, and it is apparent in the simulations reported in TO) and theory (see Eyink 1996). The fact that the magnitudes of these “counter” fluxes depend on dissipation (at small and large scales, respectively) in a different way than the “typical” (upscale energy and downscale enstrophy) fluxes is more subtle (previous reference) but also undisputed. In their numerical simulations, TO use the dependence of the downscale energy flux on the hyperviscous coefficient to control its magnitude—they choose their hyperviscous coefficient such that the resulting downscale energy flux is close to that observed in the troposphere, and in their simulation output find a transition scale that is consistent with the scale of the observed atmospheric transition from a -3 to a $-5/3$ spectral slope. Tung and Orlando (2003) interpret this independent consistency as strong support for their central claim.

There exist many published results from two-layer quasigeostrophic simulations in a channel using parameters relevant for the terrestrial midlatitudes, yet none of these studies show a transition from a -3 to $-5/3$ slope with decreasing scale. Like the model used by TO, these models employ hyperviscosity to scale selectively dissipate small-scale noise. When tuning the

Corresponding author address: K. Shafer Smith, Center for Atmosphere Ocean Science, New York University, 251 Mercer Street, New York, NY 10012.
E-mail: shafer@cims.nyu.edu

model, the hyperviscous coefficient is generally *chosen* such that the spectrum at small scales does *not* show any abrupt transitions in the inertial range near the truncation scale (this method stands in contrast to that used by TO in setting said coefficient). A spectrum that drops too sharply at intermediate to large wavenumbers, where no additional scale or forcing is imposed, is generally interpreted as the result of a too-large hyperviscous coefficient, while a spectrum that shows a bulge or transition to a shallower spectrum at small scales is interpreted as the result of a too-small hyperviscous coefficient. Furthermore, the rate of change of the spectrum at small scales, as well as the necessary magnitude of the hyperviscous coefficient are strong functions of the hyperviscous exponent s . The important fact is that the shape of the spectrum at small scales is a sensitive function of the hyperviscous coefficient and order.

Tung and Orlando (2003) invoke hyperviscosity as more than just a numerical filter, taking it as a proxy for unresolved dissipation mechanisms in the submesoscales: frontogenesis, gravity wave generation, three-dimensional boundary layer turbulence, etc. A true parameterization for dissipation due to the formation of fronts, shocks, and wave breaking must be at least nonlinear. Nevertheless, as a crude closure, hyperviscosity is sufficient to remove the enstrophy pumped downscale, and the higher the order of the filter (the exponent of the gradient operator), the more concentrated at small scales is the dissipation, yielding a wider inertial range. Moreover, assuming for the moment that hyperviscosity is relevant to the physical system (which has no short-wave cutoff), a given forcing, and ensuing downscale flux, along with a fixed hyperviscous coefficient, imply a specific dissipation scale—the equivalent of the Kolmogorov dissipation scale, adjusted for hyperviscosity (from here on this scale will be referred to as the “hyperviscous Kolmogorov,” or HVK scale). If this HVK scale is not resolved by the model, that is, if the hyperviscous coefficient is too small for the given enstrophy flux, then enstrophy will build up at the large-wavenumber end of the spectrum. While any finite hyperviscosity will ultimately dissipate the enstrophy, the large-wavenumber spectrum will be altered by the constipation of enstrophy if the HVK scale is not resolved.

Assuming only that downscale energy and downscale enstrophy fluxes begin to be affected by hyperviscous dissipation at the same scale, it is shown in section 2 that the transition scale derived by TO is coincident with the HVK scale in an infinite resolution system. It is conjectured here that the short-wave cutoff imposed by the numerical model must be “felt” by the downscale cascades in order to produce the transition scale apparent in the simulations of TO. In other words, a transition scale will only arise in a numerical simulation when the HVK scale is *smaller* than the model truncation scale, that is, when the HVK scale is unresolved. This conjecture is supported by numerical simulations that were performed with identical parameters but different res-

olutions. The results demonstrate that the transition scale found by TO changes with resolution, and in fact disappears when the HVK scale is resolved.

Interpreting as a physical phenomenon any result that is directly affected by model resolution is not common practice among modelers, or at least it is not typically acknowledged. Generally, the finite resolution of a model is considered a hindrance to understanding the physical system simulated by the model, and when possible, it is desirable to demonstrate low sensitivity to model resolution. Tung and Orlando (2003) took a different approach, and demanded that the downscale energy flux have a certain magnitude, without considering the HVK scale implied by their choice of hyperviscous coefficient and enstrophy forcing. Though they did not explicitly acknowledge the role of finite resolution in achieving their results, the present work demonstrates that finite model resolution is a prerequisite for a simulated transition scale. Thus, the proxy for the unresolved submesoscale processes implicitly used by TO is not hyperviscosity alone, but a combination of hyperviscosity and model truncation scale tuned in concert to produce a desired effect (a prechosen energy dissipation rate). Accepting the explanation of TO for the observed atmospheric spectrum demands that one believe this filter mimics the essential influence of submesoscale processes on meso- and large-scale processes, that is, that the induced energy dissipation is the only important parameter of the filter.

2. Relationship of the hyperviscous Kolmogorov scale to the transition scale

First we derive estimates of the scales at which the hyperviscosity begins to affect the downscale enstrophy and energy fluxes, thus ending their respective inertial ranges. The arguments are similar to those used to derive the Kolmogorov microscale for the direct cascade in three-dimensional turbulence (see Frisch 1995, p. 91). Consider here two-dimensional turbulence forced at wavenumber k_f and dissipated by hyperviscosity $\nu \nabla^s \zeta$, where $\zeta = \nabla^2 \psi$ is the vorticity. One should take this model as a proxy for the barotropic mode, and the forcing as a crude representation of large-scale stirring by baroclinic instability. Considering only downscale fluxes from the forcing scale, the spectral budget equation for energy is

$$\epsilon - \Pi_e(k) = 2\nu \int_{k_f}^k k'^s E(k') dk', \quad (1)$$

where $E(k)$ is the energy spectrum and ϵ is the portion of the energy flux input due to the forcing that goes *downscale* (by considering only wavenumbers $k > k_f$, we have implicitly assumed large-scale friction just balances the upscale flux of energy). The cumulative spectral energy flux $\Pi_e(k)$ goes to zero as $k \rightarrow \infty$, leaving an integral balance between forcing and dissipation. The

dissipation acts on *all* wavenumbers, but becomes increasingly significant at large wavenumber with hyperviscous dissipation. We can define a scale k_ν such that $\Pi_e(k_f < k < k_\nu^-) \simeq \epsilon$ [i.e., $\Pi_e(k)$ is constant over the inertial range, and equal to the input rate]. Above this theoretical dissipation scale, $\Pi_e(k > k_\nu) \rightarrow 0$ over some range of wavenumbers. Specifically, we can define a second wavenumber k_ν^+ such that $\Pi_e(k_\nu^+) \simeq 0$. The range of wavenumbers $k_\nu^+ - k_\nu^-$ over which the spectral flux drops off is increasingly narrow with larger hyperviscous exponent s .

To be precise, define $k_{\nu_e} = k_\nu^-$ such that $\Pi_e(k_{\nu_e}) = (1 - \gamma)\epsilon$, where $0 < \gamma \ll 1$ is an arbitrary fraction. Letting $k = k_{\nu_e}$ in (1), we limit the integration to the inertial portion of the spectrum (the smaller we choose γ , the more nearly constant is the flux over the range from k_f to k_{ν_e}). In this case one can substitute the inertial-range spectrum for $E(k)$ in (1), and further assuming that $k_f \ll k_\nu$, solve for k_ν :

$$k_{\nu_e} = a \left(\frac{\epsilon}{\nu^3} \right)^{1/(3s-2)}, \quad (2)$$

where

$$a = \left[\frac{\gamma(3s-2)}{6C} \right]^{3/(3s-2)}.$$

When the hyperviscous exponent is large, the non-dimensional prefactor a is nearly unity for the whole range of relevant parameters. As a relevant numerical example, choosing $s = 18$, $C = 6$, and $\gamma = 0.1$ yields a value of $a = 0.9$. There is an ambiguity about what value one should choose for the Kolmogorov constant C , since, for upscale energy, it is about 6, while for downscale enstrophy it is instead about $C = 1.3$ (Lindborg and Alvelius 2000). Choosing instead the latter value for C , however, also gives $a = 0.9$ (to one significant figure), and so we henceforth drop the factor a in (2.2). A similar analysis for the scale k_{ν_η} at which hyperviscosity begins to affect the downscale enstrophy flux η yields

$$k_{\nu_\eta} = b \left(\frac{\eta}{\nu^3} \right)^{1/(3s)}, \quad (3)$$

where

$$b = \left(\frac{s\gamma}{2C} \right)^{1/s}.$$

Again, $b \simeq 1$ when s is large, and so we drop it henceforth.

We now pose the hypothesis that the two scales defined by (2) and (3) must be the same. This is qualitatively obvious: since both cascading invariants are functions of some power of wavenumber times the squared amplitude of the streamfunction, the point at which streamfunction variance begins to deviate from power-law behavior is

the scale at which both invariants begin to be significantly affected by the dissipation operator. Thus, we take $k_{\nu_e} = k_{\nu_\eta} \equiv k_\nu$, and write simply

$$k_\nu = \left(\frac{\eta}{\nu^3} \right)^{1/(3s)}. \quad (4)$$

From the assumption of a single theoretical dissipation scale k_ν we can express the downscale energy flux in terms of the downscale enstrophy flux and k_ν via

$$\epsilon \simeq \eta k_\nu^{-2}. \quad (5)$$

Tung and Orlando (2003) define the transition scale as

$$k_t = \left(\frac{\eta}{\epsilon} \right)^{1/2}, \quad (6)$$

and upon substitution of (2.5) for ϵ in (2.6), we find that

$$k_t = k_\nu. \quad (7)$$

The implication here is that, at least when no short-wave cutoff is considered, there is no distinct transition scale from one inertial range to another, but rather a single scale at which the inertial range transitions to the dissipation range. Equation (4) for k_ν is an expression for this scale, and this is the expression the term hyperviscous Kolmogorov scale shall now refer to.

Note that, in the derivation above, the HVK scale was also referred to as a theoretical dissipation scale. In a numerical model in which the HVK scale is fully resolved, this scale will, in fact, also be the scale at which dissipation begins to significantly affect the downscale cascade. However, a numerical model with finite resolution and hyperviscosity run to statistically steady state will dissipate its downscale cascading invariants even when the HVK scale is not resolved, and will thus have a “dissipation scale” at which hyperviscosity begins to significantly affect the cascade that is larger than the HVK scale. In this latter case, the resulting spectral breaks are not predictable from the arguments made above.

3. Calculation of the HVK scale in the model of Tung and Orlando

Here we calculate directly, using parameters stated by TO, the HVK scales (for enstrophy and energy) and compare them to the model resolution used. Tung (2003, personal communication) reports that the hyperviscous coefficient was set relative to the Ekman friction via the following formulation:

$$\nu = 10\nu_E(\delta^2 M^2 + N^2)^{1-s/2}, \quad (8)$$

where M and N are the maximum zonal and meridional wavenumbers, respectively; $\delta = L_x/L_y$ is the aspect ratio; and ν_E is the Ekman friction coefficient. Tung and Orlando (2003) used $s = 18$, $\nu_E = (6.7 \text{ days})^{-1} = 1.7 \times 10^{-6} \text{ s}^{-1}$, $L_x = 25700 \text{ km}$, and $L_y = 3340 \text{ km}$

($\Rightarrow \delta = 0.26$) for all runs they reported. For their 129-km resolution simulation, $M = 200$ and $N = 25$. Using dimensional wavenumbers $\tilde{M} = 2\pi ML_x^{-1} = 4.5 \times 10^{-5} \text{ m}^{-1}$ and $\tilde{N} = \pi NL_y^{-1} = 2.3 \times 10^{-5} \text{ m}^{-1}$, we find that $\nu = 4.9 \times 10^{77} \text{ m}^{18} \text{ s}^{-1}$.

Tung and Orlando (2003) report $\epsilon \simeq 1 \times 10^{-6} \text{ m}^2 \text{ s}^{-3}$ and $\eta \simeq 2 \times 10^{-15} \text{ s}^{-3}$ for this same simulation. Using ν , ϵ , and η , as calculated above, in expressions (2), (3), and (6) for the HVK and transition scales, we arrive at the estimates $k_{\nu_\epsilon} = 3 \times 10^{-5} \text{ m}^{-1}$, $k_{\nu_\eta} = 3 \times 10^{-5} \text{ m}^{-1}$, and $k_\nu = 4 \times 10^{-5} \text{ m}^{-1}$, all nearly the same.

Most importantly, this HVK scale, while resolved zonally, is *not* resolved meridionally. Because the cascades of enstrophy and energy to small scales are isotropic in nature, there will be a buildup of enstrophy (and energy) along the lines (in the spectral plane) $(m, n) = (|m| < k_\nu, \pm N)$ that will affect *at least* all the wavenumbers $|\mathbf{k}| > N$. As an example, we integrate a model that is dynamically similar to the one used by TO, and show explicitly that, when k_ν is unresolved, the spectral slope at small-scale is flattened. Specifically, holding all parameters (including ν) fixed but doubling resolution leads to a change (in fact, in our case, a disappearance) of the transition scale, implying its dependence on model resolution.

4. Dependence of small-scale $-5/3$ spectrum on model resolution

The dependence (and existence) in a numerical model of the small-scale $-5/3$ spectrum on model resolution can be demonstrated explicitly. Using a two-dimensional vorticity model forced by random noise at small wavenumber $k_f = 4$, we first vary the hyperviscous coefficient about its “optimal” value, then, beginning with a lower-resolution case in which an apparent transition scale is present, double the resolution at fixed ν .

Two-dimensional vorticity dynamics mitigated by linear drag and forced at large scale by some random stirring is a simpler representation of the two-layer system considered by TO: in the two-layer version, the barotropic mode is stirred by baroclinic instability (Larichev and Held 1995), and total enstrophy cascades toward small scale while barotropic energy cascades to larger scale and is removed by the scale-independent friction. In the two-dimensional simplification, baroclinic stirring is replaced by random noise forcing F . The analogy is particularly apt at scales that are small compared to the deformation scale since, in this limit, the two-layer system decomposes into two independent two-dimensional layers. The equation is

$$\frac{\partial \zeta}{\partial t} + J(\psi, \zeta) = r\zeta + F + \nu \nabla^s \zeta, \quad (9)$$

where $\zeta = \nabla^2 \psi$. In using this equation to model the dynamics considered by TO we are ignoring the dependence of the forcing on the overall energy level. However, so long as the flow is in statistically steady

state, the spectrum at small scales does not depend on this sensitivity. This sensitivity is also ignored by TO in their analysis.

The numerical model is pseudo spectral, dealiased, doubly periodic, and only wavenumbers larger than the forcing wavenumber are dissipated by linear vorticity drag. The forcing is done with an uncorrelated white noise function that is normalized to produce an energy generation $\epsilon_0 = 1$ (see Smith et al. 2002, for details of the forcing function). This value combined with the forcing scale k_f^{-1} give a time and length scale that are used to define the other parameters of the problem. Specifically, the drag is set as $r = 0.12(\epsilon_0 k_f^2)^{1/3}$, just large enough to slow the inverse cascade (see previous reference for theory that relates r to the stopping scale).

The hyperviscous exponent is set to $s = 18$ (equivalent to $\gamma = 20$ in the formulation of TO, who define their hyperviscosity on streamfunction rather than vorticity). An optimal value of the hyperviscous coefficient is set adaptively using the smallest resolved scale as a length scale, and the inverse rms vorticity ζ_{rms} as a time scale (see e.g., Maltrud and Vallis 1991). In particular, we define

$$\nu_0 = \alpha \zeta_{\text{rms}} k_N^{-s}, \quad (10)$$

where α is a tuning factor that should be order unity for an optimal filter, and k_N is the maximum resolved wavenumber. The rms vorticity quickly settles on a nearly constant value (before even the energy is equilibrated), and so in practice the hyperviscous coefficient is nearly constant. It is shown in the appendix that (10) ensures (under reasonable assumptions) a resolved HVK scale (i.e., it ensures that $k_\nu < k_N$, when $\alpha = 1$).

The first two cases A and B both use a physical space resolution of 512^2 , which corresponds to a maximum resolved wavenumber $k_N = 255$. These cases differ only in the nondimensional factor α of expression (10), used to set the hyperviscous coefficient—in case A we set $\alpha = 1$, while in case B we set $\alpha = 0.001$. In the appendix, a theoretical estimate demonstrates that these values should lead to a resolved HVK scale for case A and an unresolved HVK scale in case B. We can also calculate the scales directly using steady-state values of the enstrophy forcing η and hyperviscous coefficient ν . The input enstrophy flux $\eta_0 = \epsilon_0 k_f^2 = 16$, but not all of the enstrophy input is fluxed downscale (just as not all of the energy input is fluxed upscale). Figure 1a shows the cumulative enstrophy fluxes $\Pi_z(k)$ for cases A and B, and from this we can estimate $\eta = \Pi_z(50 < k < 150) = 8.7$ for case A and $\eta \simeq 8.0$ for case B (the large portion of enstrophy fluxed upscale is due to the highly truncated inverse cascade inertial range). Steady-state values of the rms vorticity are $\zeta_{\text{rms}} = 10.0$ for case A and $\zeta_{\text{rms}} = 12.0$ for case B, and these values are used to calculate ν from (10). Thus, using (4) we have $k_\nu = 230$ for case A and $k_\nu = 340$ for case B. Since $k_N = 255$ for both cases, the former HVK scale is resolved while the latter is not.

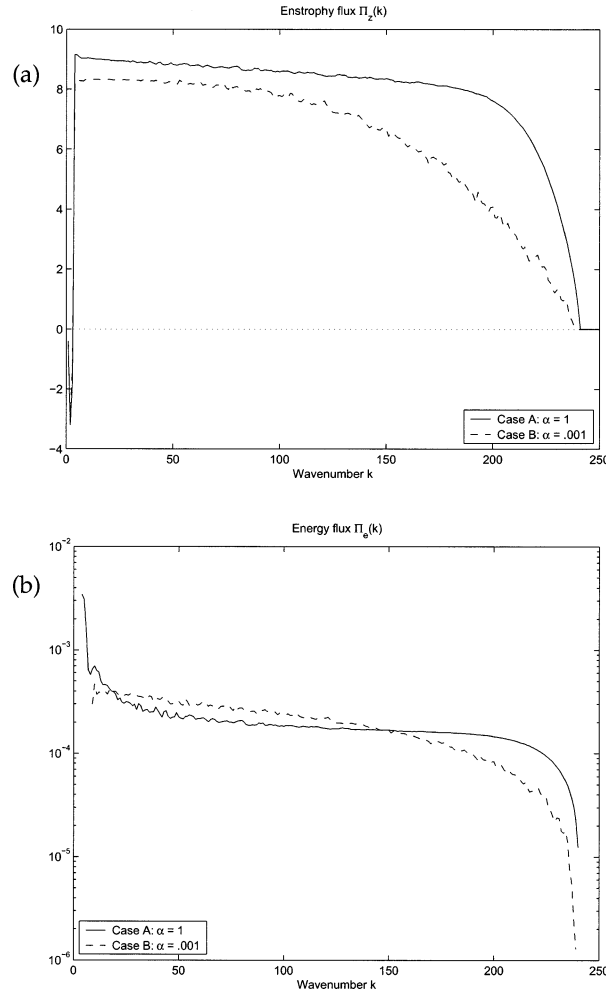


FIG. 1. (a) Cumulative enstrophy and (b) energy fluxes for cases A (solid) and B (dashed). The energy fluxes are plotted on a log scale because of their small values over the direct cascade range, and negative values above the forcing scale $k_f = 4$ are not plotted.

In Fig. 1b, we plot the downscale cumulative energy fluxes $\Pi_e(k)$. Notably, in both Figs. 1a and 1b, the inertial range assumption appears more valid for case A than case B. Averaging over the range $50 < k < 150$, we have $\epsilon = 1.9 \times 10^{-4}$ for case A, consistent with the prediction (5). For case B, the the actual energy flux is the result of an unresolved HVK scale, and thus exceeds the prediction.

Energy spectra for cases A and B, and a third case, C, are plotted in Fig. 2. The spectra are time and space averaged over the equilibrated period of each simulation. In case A the energy spectrum maintains an approximate -3 slope over most of the scales below the forcing scale, but drops off over the last 50 or so wavenumbers before the truncation scale, roughly consistent with the prediction for the HVK scale at $k_\nu = 230$. In case B the spectrum begins to flatten from a -3 slope to a $-5/3$ slope at about $k = 50$. These spectra alone demonstrate the sensitive dependence of the small-scale

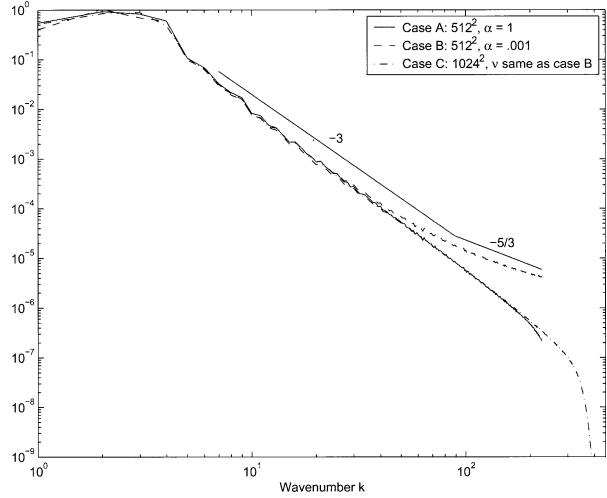


FIG. 2. Energy spectra for cases A (solid), B (dashed), and C (dashed-dotted). Cases A and B used a resolution of 512^2 and were identical except that, for case A, the hyperviscous tuning factor $\alpha = 1$, while for case B, $\alpha = 0.001$. Case C was performed at a resolution of 1024^2 , but used a hyperviscous coefficient and order identical to that of case B.

spectrum on the form and magnitude of the hyperviscous filter, and the changes that occur when the HVK scale is or is not resolved. However, barring the non-constant fluxes for case B in Fig. 1, case B could be taken as evidence for a legitimate transition scale in the present model. This argument might stand if, indeed, that transition scale remained constant using the same parameters in a higher-resolution model.

Simulation C was performed using the same parameters as case B but with double the resolution, or $k_N = 511$. The hyperviscous coefficient, though set adaptively, is made nearly identical to that for simulation B in the following way. Since the large-scale forcing is the same in both models, and knowing that, a posteriori, we will have the same ν , we can assume that the rms vorticity ζ_{rms} for each case will be nearly the same. Then equating ν_B and ν_C and using (10), we have

$$\alpha_C = \alpha_B \left(\frac{k_{N_C}}{k_{N_B}} \right)^s$$

which gives $\alpha_C = 272$. The resulting steady state for case C gives $\zeta_{\text{rms}} = 10.0$, which is slightly lower than the value 12.0 obtained for case B. However, the difference in ν for the two runs is then only 20%, which leads to negligible differences in the HVK scale, and gives $k_\nu = 340$, just as in case B. As predicted by arguments above, the once apparent transition scale disappears because the HVK scale is now resolved. Thus, at least in the model tested here, the observed transition scale is a function of model resolution.

5. Conclusions

Tung and Orlando (2003) make the valid point that a small downscale energy flux can exist in standard two-

dimensional and quasigeostrophic turbulence. They further argue that this flux will dominate the shape of the energy spectrum at sufficiently small scales. However, in the presence of linear hyperviscous dissipation and with no short-wave cutoff, the scale at which the downscale energy flux overtakes the enstrophy flux is precisely the scale at which dissipation becomes important, that is, the Kolmogorov microscale (this equivalence is due to the dependence of the downscale energy flux on the enstrophy input flux and on the hyperviscous coefficient). When the hyperviscous Kolmogorov scale is not resolved, enstrophy (and energy) will build up at the smallest scales, leading to a shallowing of the small-scale spectrum. The simulations reported by TO do not resolve the HVK scale meridionally, and this results in a shallow spectrum for all wavenumbers near to and greater than the meridional truncation wavenumber.

Tung and Orlando (2003) point out that their only criterion for the hyperviscous filtering was that the net energy dissipation affected by that filter attain a certain value. If submesoscale dissipative processes affect the mesoscale spectrum only via their net rate of energy dissipation, then TO's explanation for the $-5/3$ slope of the spectrum at small scales may be correct. The numerical tests reported by TO are consistent with this hypothesis, but the dependence of the transition scale on model resolution (due to the effect of the truncation scale on the spectrum) allows for some uncertainty. A more convincing numerical experiment could be performed with a hypothetical small-scale filter that ensured a given rate of energy dissipation at any resolution. With such a filter, one could demonstrate conclusively that the transition scale depended only on the energy dissipation rate, and not the model resolution. However, in the present absence of such a filter, the latter suggestion cannot be acted upon.

APPENDIX

Ensuring a Resolved HVK Scale

The expression for an optimal hyperviscous coefficient (10) can be related to the HVK scale (3) as follows. The root-mean-square vorticity can be expressed as

$$\zeta_{\text{rms}} = \sqrt{\int Z(k) dk},$$

where $Z(k)$ is the enstrophy spectrum. Assuming an enstrophy-flux-dominated inertial range spectrum [$Z(k) = C\eta^{2/3}k^{-1}$] from forcing scale to truncation scale, and neglecting contributions at scales larger than the forcing scale (including these contributions would only strengthen our result), this yields

$$\zeta_{\text{rms}} \simeq \eta^{1/3} \sqrt{C \ln\left(\frac{k_N}{k_f}\right)}. \quad (\text{A1})$$

Considering the HVK scale as given by (4) and using (10) for ν and (A1) for ζ_{rms} , we have

$$k_\nu = \left\{ \alpha \left[C \ln\left(\frac{k_N}{k_f}\right) \right]^{3/2} \right\}^{-1/3s} k_N. \quad (\text{A2})$$

Assuming $C \simeq 1.3$ (Lindborg and Alvelius 2000), then as long as $k_N > 2.16k_f$ (a smaller separation than the minimum necessary to get a resolved inertial range), and with $\alpha = 1$, the prefactor to k_N is less than unity. The larger the hyperviscous exponent s , the closer the factor is to unity. For our lower-resolution simulations with $k_N = 255$, and recalling that $k_f = 4$ and $s = 18$, the prefactor is 0.95 for case A ($\alpha = 1.0$) and 1.08 for case B ($\alpha = 0.001$), implying a resolved HVK scale in the former case and an unresolved HVK scale in the latter case.

REFERENCES

- Eyink, G. L., 1996: Exact results on stationary turbulence in 2D: Consequences of vorticity conservation. *Physica D*, **91**, 97–142.
- Frisch, U., 1995: *Turbulence: The Legacy of A. N. Kolmogorov*. Cambridge University Press, 296 pp.
- Larichev, V. D., and I. M. Held, 1995: Eddy amplitudes and fluxes in a homogeneous model of fully developed baroclinic instability. *J. Phys. Oceanogr.*, **25**, 2285–2297.
- Lindborg, E., and K. Alvelius, 2000: The kinetic energy spectrum of the two-dimensional enstrophy turbulence cascade. *Phys. Fluids*, **12**, 945–947.
- Maltrud, M. E., and G. K. Vallis, 1991: Energy spectra and coherent structures in forced two-dimensional and beta-plane turbulence. *J. Fluid Mech.*, **228**, 321–342.
- Nastrom, G. D., and K. S. Gage, 1985: A climatology of atmospheric wavenumber spectra of wind and temperature observed by commercial aircraft. *J. Atmos. Sci.*, **42**, 950–960.
- Smith, K. S., G. Boccaletti, C. C. Henning, I. N. Marinov, C. Y. Tam, I. M. Held, and G. K. Vallis, 2002: Turbulent diffusion in the geostrophic inverse cascade. *J. Fluid Mech.*, **469**, 13–48.
- Tung, K. K., and W. W. Orlando, 2003: The k^{-3} and $k^{-5/3}$ energy spectrum of atmospheric turbulence: Quasigeostrophic two-level model simulation. *J. Atmos. Sci.*, **60**, 824–835.